




Corpus Callosum Remodeling in Glioma: Constancy of Fiber Density and Anisotropy in MRI

Vikas Pareek , Subhadip Paul , Prasun K. Roy 

ABSTRACT: Corpus callosum (CC) is the primary fiber system bridging the cerebral hemispheres and is of critical importance for glioma migration which downgrades the prognosis. Here we present the specific pattern of CC restructuring in glioma patients. We probe that the magnetic resonance imaging-based fiber count decrease can be a ready noninvasive indicator of glioma aggressivity and prognosis. We find that to maintain the callosal neural transmission efficiency, the optimum architectural density of white matter fibers remains unchanged, even though there is gross fiber loss. This adaptation occurs by CC's isotonic restructuring, a protective compensatory behavior for maintaining CC's optimal functional efficiency despite malignant infiltration.

RÉSUMÉ : Restructuration du corps calleux dans des cas de gliome : constance de la densité des fibres et anisotropie observées lors d'examens d'IRM. Le corps calleux (CC) constitue le principal faisceau de fibres réunissant les deux hémisphères cérébraux. Il est en cela d'une importance capitale dans la migration des cellules associées aux gliomes, lesquelles affectent négativement le pronostic des patients. Nous voulons présenter ici un modèle spécifique de restructuration du CC chez des patients atteints de gliomes. Pour ce faire, nous avons exploré la possibilité qu'une diminution de la quantité de fibres observée par IRM puisse représenter un indicateur non-invasif de l'agressivité d'un gliome et d'un pronostic. Nous avons ainsi observé que le maintien de l'efficacité de la transmission neuronale du CC se traduit par une densité constitutive optimale et inchangée des fibres de la matière blanche même si cela s'accompagne d'une perte nette de fibres. Cette adaptation est survenue grâce à une restructuration isotonique du CC, comportement compensateur protecteur qui permet de maintenir l'efficacité fonctionnelle optimale du CC en dépit de l'infiltration de cellules malignes.

Keywords: Corpus callosum, Neural remodeling, Glioma, Diffusion tensor imaging, Fiber density, Fiber count, Isotonic change, Fractional anisotropy

doi:10.1017/cjn.2021.64

Can J Neurol Sci. 2022; 49: 282–286

The brain tumors and the other nervous system cancers represent the 10th leading cause of death for both genders¹; and of these tumors, the high-grade glioma (HGG) having very poor prognosis represents a fatal outcome.^{2,3} In the current study, we endeavor to explore the restructuring/remodeling which is induced in the structure of corpus callosum (CC), the evaluation being done by magnetic resonance imaging (MRI) diffusion tensor imaging (DTI) methodology. This study has recruited unilateral HGG subjects having normal appearing white matter (WM) of CC, both in the T₁-weighted, fluid-attenuated inversion recovery (FLAIR) structural image and in the fractional anisotropy (FA) map of the diffusion image. In this exploratory study, eight glioma patients (age range: 27-34 years) and eight healthy individuals (HIs) age-matched controls (age range: 27-32 years) were scanned for T₁-weighted, FLAIR and DTI acquisitions, using 3 Tesla magnetic resonance scanner (Philips Achieva 3.0 Tesla scanner at National Neuroimaging Facility, National Brain Research Centre, Manesar, India). No significant difference in the

mean ages was observed between the two groups ($p=0.07$, unpaired t test). Table 1 shows the demographic characteristics of the subjects.

For scanning, we use turbo field echo (TFE SENSE) sequence, FLAIR TSE sequence, and single-shot spin echo – echo planar imaging sequence with 32 gradient directions (with a gradient strength of 1000 s/mm²) enabling T₁-weighted, FLAIR and diffusion-weighted acquisitions, respectively. FDT (FMRIB's Diffusion Analytics platform from FMRIB Software Library [FSL]) was used for the analysis of diffusion-weighted images.⁴ Among the eight unilateral HGG subjects, one of the subjects had frontal lesion at the right hemisphere, while the other seven subjects had left hemisphere-specific gliomatic lesions. Of the seven left hemisphere-specific HGG subjects, two subjects had frontotemporal lesion, one had an occipital lesion, one had a temporal lesion, one had shown lesion spread over caudate and putamen, one with parietal lobe-associated lesion, and one with the parietotemporal lesion. Figure 1(i) shows the image analysis

From the National Neuroimaging Facility, National Brain Research Centre, Manesar, Haryana, India (VP, SP); Center for Cognitive and Brain Sciences, Indian Institute of Technology Gandhinagar, Gujarat, India (VP); Computational Neuroscience & Neuroimaging Laboratory, School of Bio-Medical Engineering, Indian Institute of Technology (I.I.T.), B.H.U., Varanasi, U.P., India (PKR); Institute of Psychiatry, Psychology & Neuroscience, King's College, London, U.K (SP); School of Biological Sciences, Ramakrishna Mission Vivekananda Education and Research Institute (RKMVERI), P.O. Belur Math, Dist. Howrah, West Bengal, India (SP); and Centre for Tissue Engineering, Indian Institute of Technology (I.I.T.), B.H.U., Varanasi, U.P., India (PKR)

RECEIVED JULY 22, 2020. FINAL REVISIONS SUBMITTED JANUARY 25, 2021. DATE OF ACCEPTANCE APRIL 5, 2021.

Correspondence to: Prasun K. Roy, Computational Neuroscience & Neuroimaging Laboratory, School of Bio-Medical Engineering, Indian Institute of Technology (I.I.T.), B.H.U., Varanasi, 222005, U.P., India. Email: pkroy.bme@iitbhu.ac.in

Table 1: Demographic particulars and site-specific details about the glioma site of the subjects

Subject category	High-grade glioma (HGG) subjects	Healthy individuals (HIs)
Total subjects recruited (<i>n</i>)	8	8
Male:Female distribution	4:4	5:3
Age (mean \pm S.D.)	31 \pm 3	29 \pm 2
Glioma site	Right hemisphere lesion: 1 (frontal lesion) Left hemisphere lesion: 7 [frontotemporal lesion (2) occipital lesion (1) temporal lesion (1) lesion spread over caudate and putamen (1) parietotemporal lesion (1) parietal lobe associated lesion (1)]	NA

*NA = Not applicable.

pipeline and Figure 1(ii) delineates the methodology that we developed for this study. For statistical analysis, unpaired *t* test was performed using Graph Pad Prism 7 version.

In the CC (Table 2), we noticed that because of glioma proliferation, a decrease was observed in both the WM fiber count and the callosal volume.^{5,6} We found 54.18% decline in the fiber count of CC in glioma subjects, compared to HI controls, the mean values for fiber count being 6.74 million and 10.39 million, respectively, and the level of significance, *p* value = 2.49×10^{-7} . The resultant effect of fiber loss is further noted as CC volume loss, where we found 51.82% loss of CC volume in glioma subjects compared to HI control, the mean values for CC volume being 10.99 and 16.62 cc, respectively, while the level of significance, *p* value = 4.88×10^{-5} . The quotient of the two parameters (fiber count and CC volume) gives the fiber density, and we noticed no differences in fiber density (*p* value > 0.05) between the glioma and normal HI subjects. Thus, the fiber density remains similar and does not alter between healthy and glioma subjects (Table 3).

When the glioma cell infiltrates in CC, there is axonal loss because of the malignant glioma-induced neuronal cell death of which a major cause is a glutamate excitotoxicity. We elucidate that the increased cellular count of the glioma lesion may induce the CC to undergo adaptive compensatory remodeling,^{7,8} whereby the fiber density does not change, even though the CC undergoes dystrophy. Consistent with the aforesaid results, we observed a significant increase (*p* = 0.03) in the mean diffusivity (MD) value of CC (Table 3 and Figure 2a) which indicates the increase in hydrous diffusion due to the rising aqueous content caused by edema and inflammation in the vicinity of glioma-infiltrative lesion in the CC.⁹

In our study, we also found that the radial diffusivity (RD) does not differ, i.e., the RD parameters do not show any significant differences (*p* = 0.06) in the glioma CC compared to the CC of HI. Since no differences were observed in RD indices between healthy subjects and glioma patients, we can elucidate that myelin

structure is intact in the CC of glioma individuals (Table 3 and Figure 2(b)). This integrity of the myelin sheath in glioma subjects is further corroborated by the fact that the myelin sheath is essential for glioma infiltration, indeed the infiltrating glioma cells need myelin for attachment and hence for using WM as scaffolds for invasion and penetration.^{10,11}

With the glioma cell infiltration in the CC, some WM tracts may lyze because of the perforins secreted by the glioma cells. Here the increased proliferating cellular population of glioma cells may induce the CC to undergo remodeling, whereby the callosal fiber density does not change, even though the CC hypotrophies or contracts due to the lessening of the number of WM tracts as a result of the glioma-induced glutamate excitotoxicity. Plausibly, to maintain the callosal transmission efficiency for the physiological functioning of the brain in glioma patients, the optimum architectural density of the WM fibers remains unchanged to adapt to the invasive glioma condition. This adaptation is enabled by the isotonic restructuring of the CC, and the restructuring being the compensatory behavior of the CC for maintaining its optimal functional efficiency in spite of malignant glioma cell infiltration.

Collateral investigations, using MRI and histological/cytological autopsy studies, indicate that in the CC (whether in a healthy condition or with neuroinflammatory disease) one observes that the FA characterizes the WM fiber density, instead of myelination deficit or axonal damage. That is, in the CC, higher the WM density, more the FA.^{12,13} The above observation is also corroborated in glioblastoma; for instance, the fiber density index strongly correlates with the values of FA in the normal-appearing WM and in the perilesional WM.¹⁴ In our glioma case, we have detected that the callosal fiber density does not change when compared to the HIs. Hence, we can infer from the earlier statements that callosal FA in glioma subjects should not differ from HIs. This prediction is indeed well corroborated by our study showing no differences in the FA evaluations (*p* = 0.43) (Table 3 and Figure 2(c)).

Furthermore, an important aspect is the quantitative significance and implication of the decrease in callosal fiber count in glioma. The fiber count in the CC decreases on an average from 10.39 million (normal controls) to 6.74 million (in glioma) (Table 2), indicating a 35% decrease in the tract number. One knows histopathologically that glioma cells gradually destroy and replace neuronal cells.¹⁵ It is known that the percentage decrease in DTI fiber count directly and linearly correlates with the intensity of malignant aggressivity of a glioma tumor (*r* = 0.83), the tumor aggressivity being estimated by the Mindbomb E3 ubiquitin protein ligase 1 (MIB-1) index of a tumor.¹⁶ The MIB-1 staining technique is an antibody-based assay that acts on the glioma cell's Ki-67 antigen, which is expressed in mitotic and nonresting phases of the cell and is an indicator of cell division and proliferation intensity. Hence, regarding the glioma patients, we can posit that the amount of decrease in fiber count (with respect to the average fiber count of HIs) may be taken as an indicator of the aggressivity and prognosis of glioma.

In conclusion, our MRI-DTI-based investigation of glioma patients furnishes an unique insight on the nature of isotonic restructuring of CC in gliomatic invasion, leading to loss in fiber count numbers but maintaining the fiber density of CC in

Table 2. Corpus callosum (CC) volume and fiber count for healthy individuals and glioma subjects

CC volume (cm ³)	Healthy individuals (HIs)							
		15.75	15.58	17.93	15.88	18.70	17.14	14.50
Glioma subjects								
	6.41	13.45	9.16	13.57	10.7	12.29	11.71	10.65
Fiber count (n)	Healthy individuals (HIs)							
	9.84×10^6	9.73×10^6	1.12×10^7	9.92×10^6	1.17×10^7	1.07×10^7	9.1×10^6	1.1×10^7
Glioma subjects								
	6.65×10^6	7.32×10^6	7.68×10^6	6.69×10^6	5.57×10^6	7.09×10^6	6.9×10^6	5.9×10^6

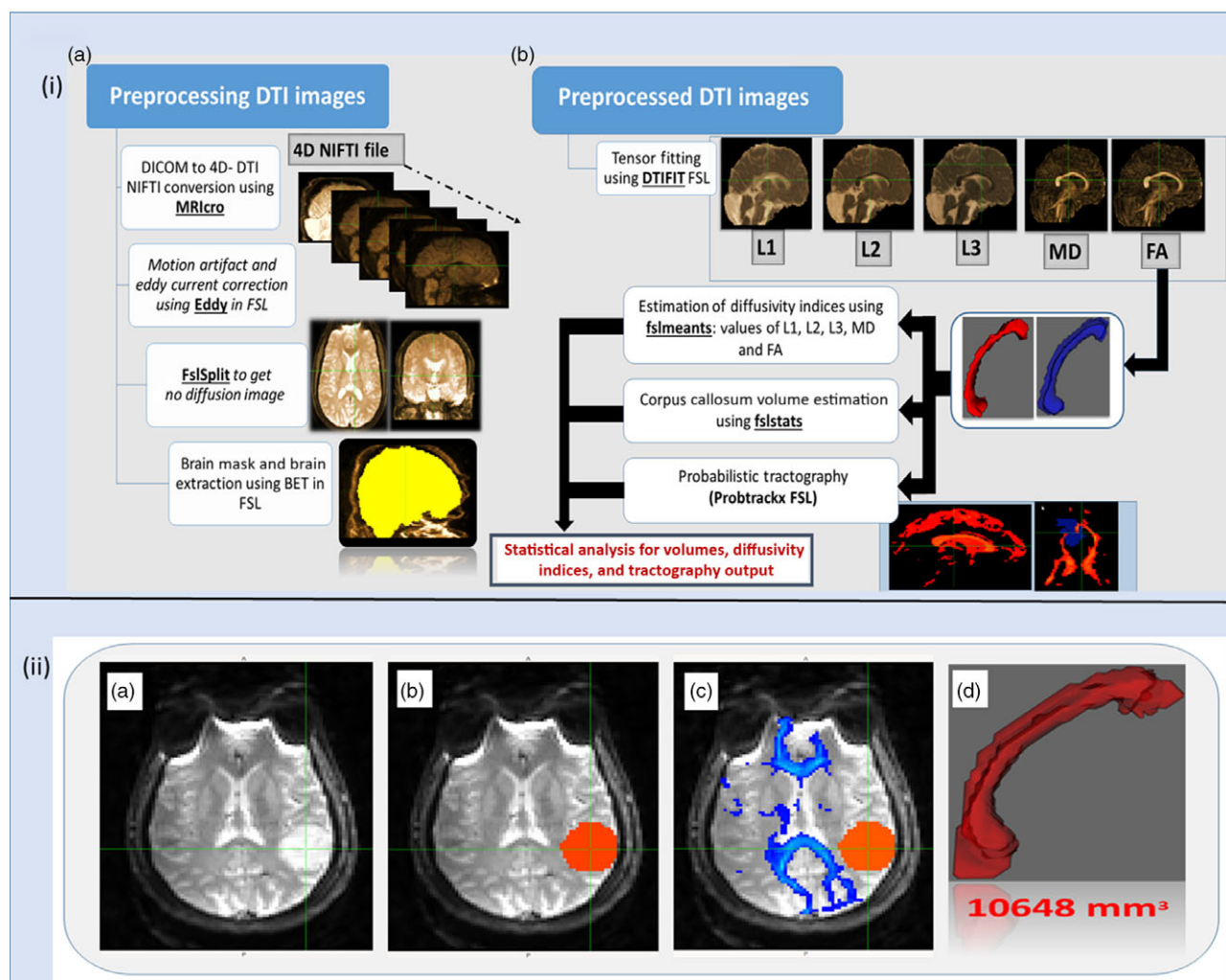


Figure 1: Image analysis pipeline and Methodology of the Imaging Analysis procedure. (i) Image analysis pipeline: (a) Preprocessing DTI images, and (b) Post-Processing of Preprocessed DTI images for Diffusivity Indices estimation, Corpus Callosum Volume estimation, and performing Probabilistic tractography. (ii) Methodology of the Imaging Analysis procedure: (a) Diffusion-Weighted Image of the brain showing the tumour; (b) For the glioma lesion, the Tumour Mask (red) is constructed from the FA map; (c) Fiber tractography is formulated and visualized for the Corpus Callosum (blue); (d) Creation of the Corpus Callosum's region of interest (red) for the waypoint mask (mid-sagittal view). The volume (in ml) derived from this mask is shown as the numerical value.

glioma subjects (so as to be at the same level as fiber density of normal subjects). Further, we elucidate that the FA may be taken to be a potential imaging biomarker representing the fiber density for glioma patients. The increase in MD in glioma CC reflects the

effect of inflammation, which is associated with edema induced by extracellular matrix degrading metalloproteinases^{17,18} which is enhanced by the mutation of tumor suppressor protein (related to *p53* gene).

Table 3: Statistical differences and p values for fiber density, diffusivity indices, and anisotropic measurements (radial diffusivity, mean diffusivity, and fractional Anisotropy)

Fiber density and diffusivity indices	t	df	p Value	p Value summary	R^2 (eta square)	Glioma effect ($p < 0.05$)
Fiber density	0.3013	14	0.7675	ns	0.006444	×
Radial diffusivity	2.009	14	0.0643	ns	0.2237	×
Mean diffusivity	2.435	14	0.0289	*	0.2975	↑
Fractional anisotropy	0.88173	14	0.4274	ns	0.04555	×

(ns = not significant; * indicates $p < 0.05$).

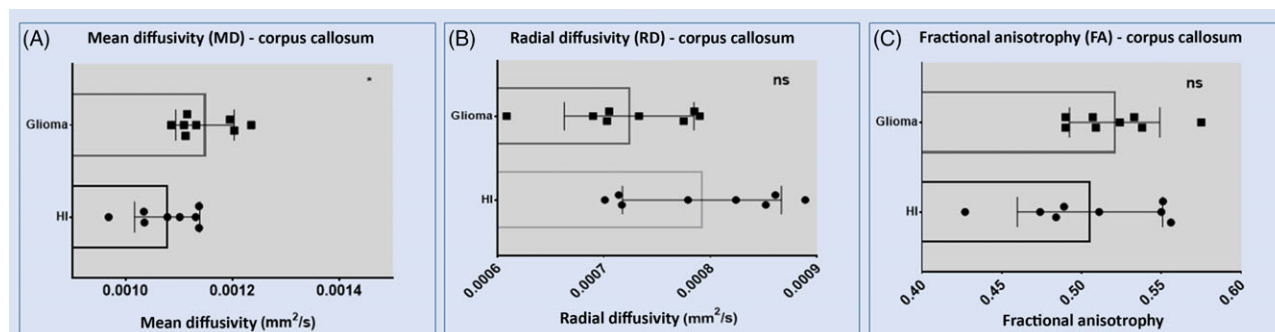


Figure 2: Comparison of Corpus Callosum parameters in glioma subjects and healthy individuals: Diffusivity indices and Anisotropy measurements: (A) Mean Diffusivity (MD), (B) Radial Diffusivity (RD), and (C) Fractional Anisotropy (FA) (p -value summary, ns: >0.05 , *: <0.05).

Additionally, we have observed that in CC, the RD does not significantly change between glioma subjects and normal controls. From conjoint MRI and histology studies of CC of preclinical investigations,^{10,19} it is well-known that alteration of RD well correlates with the level of myelin damage. These studies indicate that if RD does not change, then myelin damage may not have occurred. Hence, our observation that RD does not alter in glioma implies that myelin damage in CC may not be significant in glioma (even though there is edema, as mentioned before).

One of the limitations of our investigation is the constrained sample size of HGG subjects. In the future studies, it may be worthwhile to enhance the sample size and recruit the glioma subjects comprising significant numbers for each subset based on the lesion site (e.g., gliomas in the frontal lobe, parietal lobe, occipital lobe, etc.). The microscopic examinations of the CC is needed to be performed postoperatively in future investigations, for validating and further extending the observations made in the current study.

ACKNOWLEDGMENTS

Appreciation is extended to the Indian Institute of Technology (B.H.U.)–Varanasi and to the National Brain Research Centre–Manesar for providing institutional facilities.

FUNDING

The research is aided by the Dept. of Science & Technology (program of National Mission on Data Analytics & Predictive Technologies, National Mission on Interdisciplinary Cyber-Physical

Systems), under the Ministry of Science & Technology, Govt. of India.

CONFLICT OF INTEREST

The authors declare that they have no conflicts of interest.

STATEMENT OF AUTHORSHIP

VP, SP, and PKR conceived and designed the experiments. VP and PKR analyzed the data. VP and PKR wrote the first draft of the manuscript. VP, SP, and PKR contributed to the writing of the manuscript. VP, SP, and PKR agreed with manuscript results and conclusions. VP and PKR jointly developed the structure and arguments for the paper. VP, SP, and PKR made critical revisions and approved final version. All authors reviewed and approved the final manuscript.

INFORMED CONSENT

Informed consent was obtained from all individual participants included in the study.

ETHICAL APPROVAL

All procedures performed in studies involving human participants were in accordance with the ethical standards of the institutional and/or national research committee and with the 1964 Helsinki declaration and its later amendments or comparable ethical standards.

REFERENCES

1. Brain Tumor: Statistics | Cancer. Available at: <https://www.cancer.net/cancer-types/brain-tumor/statistics#:~:text=Brain%20tumors%20account%20for%2085,about%20brain%20tumors%20in%20children>.
2. Mirimanoff RO. High-grade gliomas: Reality and hopes. *Chin J Cancer*. 2014;33:1–3.
3. MacDonald TJ, Aguilera D, Kramm CM. Treatment of high-grade glioma in children and adolescents. *Neuro Oncol*. 2011;13:1049–1058.
4. Smith SM, Jenkinson M, Woolrich MW, et al. Advances in functional and structural MR image analysis and implementation as FSL. *Neuroimage*. 2004;23:S208–S219.
5. Roberts TPL, Liu F, Kassner A, Mori S, Guha A. Fiber density index correlates with reduced fractional anisotropy in white matter of patients with glioblastoma. *AJNR Am J Neuroradiol*. 2005;26:2183–2186.
6. Pareek V, Paul S, Rallabandi VPS, Roy PK. Patterning of corpus callosum integrity in glioma observed by MRI: Effect of 2D bi-axial lamellar brain architecture. *J Neurooncol*. 2019;144:165–177.
7. Ye ZC, Sontheimer H. Glioma cells release excitotoxic concentrations of glutamate. *Cancer Res*. 1999;59:4383–4391.
8. Eyüpoglu IY, Hahnen E, Heckel A, et al. Malignant glioma-induced neuronal cell death in an organotypic glioma invasion model. *J Neurosurg*. 2005;102:738–744.
9. Hetherington H, Bandak A, Ling G, Bandak FA. Advances in imaging explosive blast mild traumatic brain injury. *Handb Clin Neurol*. 2015;127:309–318.
10. Winkiewski PJ, Sabisz A, Naumczyk P, Jodzio K, Szurowska E, Szarmach A. Understanding the physiopathology behind axial and radial diffusivity changes - what do we know? *Front Neurol*. 2018;9:92.
11. Giese A, Kluwe L, Laube B, Meissner H, Berens ME, Westphal M. Migration of human glioma cells on myelin. *Neurosurgery*. 1996;38:755–764.
12. Wahl M, Lauterbach-Soon B, Hattingen E, et al. Human motor corpus callosum: topography, somatotopy, and link between microstructure and function. *J Neurosci*. 2007;27:12132–12138.
13. Hofer S, Frahm J. Topography of the human corpus callosum revisited—comprehensive fiber tractography using diffusion tensor magnetic resonance imaging. *Neuroimage*. 2006;32:989–994.
14. Roberts TPL, Liu F, Kassner A, Mori S, Guha A. Fiber density index correlates with reduced fractional anisotropy in white matter of patients with glioblastoma. *AJNR Am J Neuroradiol*. 2005;26:2183–2186.
15. Scherer HJ. Structural development in gliomas. *Am J Cancer*. 1938;34:333–351.
16. Campanella M, Ius T, Skrap M, Fadiga L. Alterations in fiber pathways reveal brain tumor typology: a diffusion tractography study. *PeerJ*. 2014;2014.
17. Ham SW, Jeon H-Y, Jin X, et al. TP53 gain-of-function mutation promotes inflammation in glioblastoma. *Cell Death Differ*. 2019;26:409–425.
18. Nakada M, Okada Y, Yamashita J. The role of matrix metalloproteinases in glioma invasion. *Front Biosci*. 2003;8:e261–9.
19. Song SK, Yoshino J, Le TQ, et al. Demyelination increases radial diffusivity in corpus callosum of mouse brain. *Neuroimage*. 2005;26:132–140.